

Published in final edited form as:

Ophthalmology. 2012 November ; 119(11): 2261–2269. doi:10.1016/j.ophtha.2012.06.009.

Diagnosing Preperimetric Glaucoma with Spectral Domain Optical Coherence Tomography

Renato Lisboa, M.D.^{1,2}, Mauro T. Leite, M.D.², Linda M. Zangwill, Ph.D.¹, Ali Tafreshi, B.S.¹, Robert N. Weinreb, M.D.¹, and Felipe A. Medeiros, M.D., Ph.D.¹

¹Hamilton Glaucoma Center and Department of Ophthalmology, University of California, San Diego

²Federal University of São Paulo, Department of Ophthalmology, Brazil

Abstract

Purpose—To evaluate the diagnostic accuracy of spectral domain optical coherence tomography (SDOCT) for detection of preperimetric glaucoma and compare it to the performance of confocal scanning laser ophthalmoscopy (CSLO).

Design—Cohort study.

Participants—A cohort of 134 eyes of 88 patients suspected of having glaucoma based on the appearance of the optic disc.

Methods—Patients were recruited from the Diagnostic Innovations in Glaucoma Study (DIGS). All eyes underwent retinal nerve fiber layer (RNFL) imaging with Spectralis SDOCT and topographic imaging with HRT-III CSLO within 6 months of each other. All patients had normal visual fields at the time of imaging and were classified based on history of documented stereophotographic evidence of progressive glaucomatous change in the appearance of the optic nerve occurring before the imaging sessions.

Main Outcome Measures—Areas under the receiver operating characteristic curves (AUC) were calculated to summarize diagnostic accuracies of the SDOCT and CSLO. Likelihood ratios (LRs) were reported using the diagnostic categorization provided by each instrument after comparison to its normative database.

Results—Forty-eight eyes of 42 patients had evidence of progressive glaucomatous change and were included in the preperimetric glaucoma group. Eighty-six eyes of 46 patients without any evidence of progressive glaucomatous change followed untreated for an average of 14.0 ± 3.6 years were included in the control group. The parameter with the largest AUC obtained with the

© 2012 American Academy of Ophthalmology, Inc. Published by Elsevier Inc. All rights reserved.

Financial Disclosure(s):

The author(s) have made the following disclosure(s):

Renato Lisboa – None

Mauro T. Leite – None

Linda M. Zangwill – Financial support – Carl-Zeiss Meditec Inc, Heidelberg Engineering

Ali Tafreshi – None

Robert N. Weinreb – Financial support – Alcon, Allergan, Merck, Baush & Lomb, Zeiss Meditec, Optovue, Novartis, Nidek, Topcon, Aeries

Felipe A. Medeiros – Financial support – Carl-Zeiss Meditec, Inc; Heidelberg Engineering, GmBH

Publisher's Disclaimer: This is a PDF file of an unedited manuscript that has been accepted for publication. As a service to our customers we are providing this early version of the manuscript. The manuscript will undergo copyediting, typesetting, and review of the resulting proof before it is published in its final citable form. Please note that during the production process errors may be discovered which could affect the content, and all legal disclaimers that apply to the journal pertain.

SDOCT was the temporal superior RNFL thickness (0.88 ± 0.03), followed by global RNFL thickness (0.86 ± 0.03) and temporal inferior RNFL thickness (0.81 ± 0.04). The parameter with the largest AUC obtained with the CSLO was rim area (0.72 ± 0.05), followed by rim volume (0.71 ± 0.05) and linear cup to disk ratio (0.66 ± 0.05). Temporal superior RNFL average thickness measured by SDOCT performed significantly better than rim area measurements from CSLO (0.88 vs. 0.72; $p = 0.008$). Outside normal limits results for SDOCT parameters were associated with strongly positive LRs.

Conclusions—RNFL assessment with SDOCT performed well in detecting preperimetric glaucomatous damage in a cohort of individuals suspected of having the disease and had a better performance than CSLO.

INTRODUCTION

Clinicians are frequently faced with the challenge of diagnosing glaucoma in patients who present with optic discs that have suspicious findings for the disease, such as apparent enlarged cupping or neuroretinal rim thinning, but in whom clinical examination at the slit-lamp or using optic disc photographs is inconclusive. In the presence of normal visual field tests, clinicians may complement their evaluation by ordering additional diagnostic tests, such as quantitative evaluation of the optic nerve or retinal nerve fiber layer with imaging instruments. The results obtained from imaging evaluation can assist clinicians in deciding whether or not preperimetric glaucomatous optic neuropathy is present and in establishing treatment and follow-up plans.

The introduction of spectral domain optical coherence tomography (SDOCT) has resulted in improved imaging resolution and reproducibility compared to previous versions of this technology,^{1, 2} offering the potential for improved assessment of structural damage in glaucoma. Although several studies have been reported evaluating the diagnostic accuracy of imaging devices in glaucoma, the design of most studies has not replicated the situation in which these tests are used in clinical practice. Most studies have been performed by comparing the ability of imaging devices to discriminate patients with confirmed glaucomatous visual field loss from healthy individuals in a cross-sectional design.^{3–21} However, it should be obvious that the presence of visual field loss by itself would obviate the need for using an imaging instrument to diagnose the disease in clinical practice. In fact, a clinician is most interested in the ability of a test to provide additional information that can be helpful in a patient who presents suspicious findings for the disease, as described above.

The conduct of studies evaluating glaucoma suspects and for detection of preperimetric damage has been limited by the inexistence of a perfect reference standard that could be used to diagnose disease at a single point in time without relying on visual fields. However, longitudinal follow-up can be used to evaluate the existence of progressive structural damage, which would then confirm the diagnosis.^{22–25} The final diagnosis based on longitudinal follow-up can then be used as a reference standard with which the results of the imaging instruments are to be compared.

The purpose of this study was to evaluate the diagnostic accuracy of retinal nerve fiber layer (RNFL) with Spectralis SDOCT for detection of preperimetric glaucomatous damage in patients suspected of having the disease. In addition, we compared the diagnostic ability of the SDOCT technology with the diagnostic ability of optic disc topographic measurements obtained by confocal scanning laser ophthalmoscopy (CSLO). We used longitudinal information to establish the final diagnosis in these patients and as a reference standard for comparison of results.

METHODS

Participants

This was an observational cohort study which included patients recruited from the Diagnostic Innovations in Glaucoma Study (DIGS) conducted at the Hamilton Glaucoma Center (University of California, San Diego). As part of DIGS, participants were prospectively evaluated according to a pre-established protocol that included visits with a comprehensive clinical examination and several imaging and functional tests. All participants who met the inclusion criteria described below were enrolled and all data were entered in a computer database. Informed consent was obtained from all participants. The University of California San Diego Human Subjects Committee approved all protocols, and methods described attended to the tenets of the Declaration of Helsinki.

Each subject underwent a comprehensive ophthalmic examination, including review of medical history, best corrected visual acuity (BCVA), slit-lamp biomicroscopy, intraocular pressure (IOP) measurement using Goldmann applanation tonometry, gonioscopy, dilated funduscopy examination using a 78-diopter (D) lens, stereoscopic optic disc photography, and standard automated perimetry (SAP) with 24-2 Swedish Interactive Threshold Algorithm (Carl Zeiss Meditec, Inc., Dublin, CA).

To be included subjects had to have best corrected visual acuity of 20/40 or better, spherical refraction less than ± 5.0 D, cylinder correction less than ± 3.0 D and open angle with gonioscopy. Subjects with coexisting retinal disease, uveitis or non-glaucomatous optic disc neuropathy were excluded from the study.

A cohort of participants suspected of having glaucoma was selected from our DIGS database. These participants were selected based on the presence of suspicious appearance of the optic nerve from cross-sectional evaluations of stereophotographs at the time of imaging by 2 independent masked graders. A third experienced grader reviewed the photographs in case of disagreement. Features characteristic of suspicious glaucomatous appearance of the optic disc were neuroretinal rim thinning, cupping, or suspicious RNFL defects. All participants had a normal SAP visual field result at the time of imaging. A normal visual field was defined as a mean deviation and pattern standard deviation within 95% confidence limits and a glaucoma hemifield test result within normal limits. Additionally, participants did not have evidence of repeatable glaucomatous visual field loss before the date of their examination with imaging instruments. All participants had been previously followed for at least 5 years before their imaging session.

These participants were then classified based on previous history of documented evidence of progressive glaucomatous change in the appearance of the optic disc occurring before the imaging sessions. Patients with documented evidence of progressive glaucomatous nerve damage at any time before both imaging sessions with SDOCT and CSLO were considered as having preperimetric glaucoma. Progressive glaucomatous change in the appearance of the optic disc was assessed by simultaneous stereoscopic photographs (TRC-SS, Topcon Instrument Corp. of America, Paramus, NJ). Stereoscopic sets of slides were examined using a stereoscopic viewer (Asahi, Pentax, Tokyo, Japan). The photographs were evaluated by 2 experienced graders, and each was masked to the subject's identity, to other tests results and to the chronological sequence of the photographs. For inclusion, photographs needed to be graded adequate or better. Definition of change was based on focal or diffuse thinning of the neuroretinal rim, increased excavation, or enlargement of the RNFL defects. Changes on rim color, presence of disc hemorrhages, or progressive parapapillary atrophy were not sufficient for characterization of progression. Discrepancies between the 2 graders were resolved by either consensus or adjudication of a third experienced grader.

A total of 48 eyes of 42 participants with progressive optic disc damage and no visual field loss were included in the preperimetric glaucoma group. These subjects were followed for an average of 14.9 ± 4.2 years.

A total of 86 eyes of 46 patients followed untreated for 14.0 ± 3.6 years without any evidence of progressive change in the appearance of the optic disc or visual field loss were used as the control group.

Instrumentation

The Spectralis SDOCT (software version 5.3.3.0, Heidelberg Engineering, Dossenheim, Germany) was used to obtain RNFL thickness measurements. Details of its operation have been published elsewhere.²⁶ The high-resolution protocol was utilized, obtaining 1536 A-scans from a 3.45mm circle centered at the optic disc, providing an axial resolution of 3.9 μm and a lateral resolution of 6 μm . The examiner was required to manually place the scan around the optic disc. To increase the image quality the Spectralis SDOCT includes an automatic real time function that gathers multiple frames (B-scans). The images were then averaged for noise reduction. The standard deviation of the signal-to-noise ratio was available to the examiner, enabling the assessment of the signal's acceptability. The quality scores ranges from 0dB (poor) to 40dB (excellent). To be included, all images were reviewed by experienced staff of the Imaging Data Evaluation and Assessment (IDEA) Center for non-centered scans, accurate segmentation and had to have a signal strength > 15dB. The parapapillary RNFL thickness sectors evaluated in this study were temporal quadrant (316 – 45 degrees), temporal superior quadrant (46 – 90 degrees), nasal superior quadrant (91 – 135 degrees), nasal quadrant (136 – 225 degrees), nasal inferior quadrant (226 – 270 degrees) and temporal inferior quadrant (271 – 315 degrees).

For each parameter, the Spectralis SDOCT software provides a classification (within normal limits, borderline and outside normal limits) based on the comparison with an internal normative database of 201 healthy eyes of Caucasian patients. The parameter is classified as within normal limits if its value falls within the 95% confidence interval (CI) of the healthy, age-matched population. A borderline result indicates that the value is between the 99% and 95% CI, and an outside normal limits result indicates that the value is lower than the 99% CI. This classification is provided in the Spectralis SDOCT printout using a color-coded pattern where within normal limits, borderline and outside normal limits are represented in green, yellow and red, respectively. The software also provides an overall classification. A normal overall classification requires all sectors and the global thickness to be within normal limits. A borderline result occurs when at least one sector or the global thickness is classified as borderline, and an outside normal limit result is provided if at least one sector or the global thickness is outside normal limits. Likelihood ratios (LRs) were calculated for each parameter and each possible diagnostic categorization (within normal limits, borderline and outside normal limits), as provided by the Spectralis SDCT software.

The HRT-III (Heidelberg Explorer Software version 1.5.10.0, Heidelberg Engineering, Dossenheim, Germany) was used to acquire CSLO images in the study. It uses confocal scanning laser principles to obtain a 3-dimensional topographic image of the optic nerve. For each patient, 3 topographical images were obtained, combined, and automatically aligned to make a single mean for topography for analysis. Magnification errors were corrected using patients' corneal curvature measurements. An experienced examiner outlined the optic nerve margin on the mean topographic image while viewing stereoscopic photographs of the optic disc. Good images required a focused reflectance image with a standard deviation not greater than 50 μm , as determined by experienced reviewers from the IDEA Center.

Topographical parameters provided by the HRT-III software and investigated in this study were rim area, rim volume, linear cup-to-disk ratio, cup-to-disk area ratio, rim-to-disk area ratio, RNFL cross sectional area, mean RNFL thickness, cup area, cup volume and mean cup depth. The global glaucoma probability score (GPS) was also evaluated as a diagnostic variable in this study. This score uses an automated analysis for the detection of glaucomatous damage that does not require the user to draw a contour line around the optic disc and does not use a reference plane. It is based on a 3-D model of the entire topographical image, including the optic disc and surrounding peripapillary RNFL. The development of this parameter is based on the work of Swindale et al.²⁷

The software for the HRT-III also incorporates the Moorfields Regression Analysis (MRA),²⁸ which compares the patient's rim area with a predicted rim area for a given disc area and age, based on confidence limits of a regression analysis derived from 627 normal patients (452 Caucasians, 111 African Origin and 64 Indians). Each sector and the global rim area are classified as within normal limits if the measurement is within the 95% CI, borderline if the measurements is between the 99.9% and 95% CI, and outside normal limits if the measurements is lower than the 99.9% CI. The MRA also provides an overall classification. A normal overall classification requires all sectors and the global rim area to be within normal limits. A borderline result occurs when at least one sector or the global rim area is classified as borderline, and an outside normal limit result is provided if at least one sector or the global rim area is outside normal limits. LRs were calculated for each possible diagnostic categorization (within normal limits, borderline and outside normal limits) of the global and sectoral results as well as for the overall classification of the MRA.

Statistical Analysis

Descriptive statistics included mean and standard deviation for normally distributed variables and median, first quartile and third quartile for non-normally distributed variables.

Areas under the receiver operating characteristic curves (AUC) were calculated to summarize the diagnostic accuracy for each parameter. An AUC equal to 1 represents perfect discrimination, whereas an AUC of 0.5 represents chance discrimination. The pairwise comparison of the AUCs was performed for each parameter using a method proposed by Dodd and Pepe.²⁹ A bootstrap resampling procedure ($n = 1000$ resamples) was used to derive the confidence intervals.³⁰ Sensitivity at fixed specificities of 80% and 95% were also reported for each parameter of each instrument. To account for potential correlation between eyes, the cluster of the data for the study subject was considered as the unit of resampling when calculating standard errors. This procedure has been used to adjust for the presence of multiple correlated measurements of the same unit.^{30, 31}

Diagnostic categorization (within normal limits, borderline or outside normal limits) provided by each instrument after comparison with its normative database was used to calculate LRs. LR is defined as the probability of a given test result in those with disease divided by the probability of the same test result in those without disease.^{32, 33} Once determined, a LR can be directly incorporated into the calculation of posttest probability of disease by using the formulation of the Bayes' theorem.³⁴ The LR for a given test result indicates how much that result will raise or decrease the pretest odds of disease. Application of LRs in the interpretation of results of imaging instruments for glaucoma diagnosis has been detailed previously.^{6, 24} A value of 1 means that the test provides no addition information, and ratios higher or lower than 1 increase or decrease the likelihood of disease, respectively.

A classification of impact of LRs of various magnitudes on posttest probability of disease has been suggested and was used in our study.³³ According to this classification, LRs

greater than 10 or lower than 0.1 would be associated with large effects on posttest probability, LRs from 5 to 10 or from 0.1 to 0.2 would be associated with moderate effects, LRs from 2 to 5 or from 0.2 to 0.5 would be associated with small effects, while LRs closer to 1 would be insignificant. Confidence intervals (CI) of 95% for LRs were calculated according to the method proposed by Simel and associates.³⁵

All statistical analyses were performed with commercially available software (Stata version 11, StataCorp, College Station, TX). The alpha level (type I error) was set at 0.05.

RESULTS

Table 1 shows demographic and clinical characteristics for the eyes included in the study. No difference in age, gender or ancestry was found between the groups.

Table 2 shows mean values of SDOCT parameters in the glaucoma and control groups. Glaucomatous eyes had, on average, significantly thinner RNFL measurements compared to the control group. The parameters with the largest AUCs were temporal superior thickness (0.88 ± 0.03), global thickness (0.86 ± 0.03) and temporal inferior thickness (0.81 ± 0.04). Figure 1 shows receiver operating characteristic (ROC) curves for these parameters.

Table 3 presents LRs with 95% CIs for the Spectralis SDOCT after comparison with the instrument's normative database. For all parameters an outside normal limits result was associated with large effects on the posttest probability of disease, except for nasal superior thickness, which was associated with moderate effects. The effect on posttest probability for borderline results ranged from insignificant to large. Within normal limits results were associated with small to insignificant effects on posttest probability of disease. An outside normal limits result in the overall Spectralis SDOCT classification was associated with a large effect on the posttest probability (LR = 50.16), whereas a borderline result was associated with an insignificant (LR = 1.05) effect and a within normal limits result was associated with small (LR = 0.26) effect on the posttest probability of disease.

Table 4 shows mean values of CSLO parameters in glaucoma and control groups. Statistically significant differences between the glaucoma and control groups were found for most parameters, except for mean cup depth. Table 4 also shows the AUC for each parameter. The parameters with the largest AUCs were rim area (0.72 ± 0.05), rim volume (0.71 ± 0.05) and linear cup-to-disk ratio (0.66 ± 0.05). The contour line-independent parameter global GPS had an AUC of $0.64 (\pm 0.05)$. Figure 2 shows the ROC curves for rim area, rim volume and global GPS of the CSLO.

Table 5 presents LRs with 95% CIs for the HRT-III MRA. Outside normal limits results were generally associated with small or insignificant effects on the posttest probability of disease, except for the temporal inferior sector that was associated with large effect (LR = 17.91). Borderline and within normal limits results were associated with insignificant to small effects. For the overall classification, both an outside normal limit result (LR = 3.19) as well as a within normal limit result (LR = 0.42) were associated with small changes in the probability of disease. A borderline result was associated with insignificant change in the probability of disease (LR = 0.82).

The SDOCT parameter with largest AUC, temporal superior RNFL thickness, performed significantly better than the CSLO parameter with largest AUC, rim area (0.88 vs. 0.72 $p = 0.008$, respectively), for differentiating between the preperimetric glaucoma and control groups. Table 6 shows the comparison of the diagnostic accuracy of SDOCT RNFL thickness parameters with the best performing CSLO parameter (rim area), according to the sectors around the optic disc. Statistical comparison of AUCs between instruments showed

significant differences between SDOCT RNFL thickness and CSLO rim area for the temporal superior (0.88 vs 0.68; $p = 0.001$, respectively) and temporal inferior (0.81 vs 0.64; $p = 0.01$, respectively) sectors. Figure 3 shows ROC curves of the temporal superior average RNFL thickness measured by the SDOCT and the temporal superior rim area measured by the CSLO.

DISCUSSION

The present study demonstrated that RNFL assessment with Spectralis SDOCT was able to detect preperimetric glaucomatous damage in eyes suspected of having the disease. In addition, SDOCT performed better than topographic optic disc assessment obtained with CSLO. These findings may have significant implications for the use of SDOCT technology as an ancillary test in the diagnostic evaluation of patients suspected of having glaucoma.

Several studies have investigated the ability of SDOCT to detect glaucomatous damage. In previous investigations, the diagnostic accuracy usually was assessed based on the ability of the tested parameters to differentiate eyes with repeatable glaucomatous visual field loss from those of healthy subjects.^{11, 12, 17-21} Such investigations are important to provide an initial assessment of the ability of the instrument to detect damage. In other words, if the instrument fails to separate these two clearly distinct groups, it would generally be regarded as not useful for diagnostic purposes. However, in clinical practice, a diagnostic test is used to diagnose disease in patients suspected of having it, not in patients with confirmed diagnosis. Therefore, if a test succeeds in initial diagnostic studies, further steps are needed to evaluate whether it is able to provide clinically relevant information. The evaluation of the ability of imaging devices to provide additional information besides that of clinical examination and visual field testing is fundamental in order to measure their true value as complementary tests for diagnosing glaucoma in suspected patients. The design of our study enabled the evaluation of the performance of these tests in the clinically relevant situation of diagnosing disease in patients with suspicious appearance of the optic disc.

Our estimates of diagnostic accuracy were generally lower than those reported by studies investigating only patients with glaucomatous visual field loss.^{3-9, 11-13, 16-21} Leung et al¹⁹ compared SDOCT and CSLO in discriminating eyes with glaucomatous visual field damage from those of healthy subjects and found AUC of 0.978 for the SDOCT parameter global RNFL thickness. In our study, we found a corresponding AUC of 0.86. A reasonable explanation for such different findings is that the accuracy of diagnostic instruments can vary according to the cohort investigated and the reference standard used to define disease.³⁶ The lower performance of the imaging instruments in our study compared to previous ones is probably related, at least in part, to the less severe stage of disease in glaucoma patients included in our analyses. As the patients did not have visual field damage at the time of imaging, they were likely at an earlier stage of disease than those included in previous studies using patients with visual field damage. Furthermore, the worse performance is also likely related to the method of selection of the control group. In our study, control subjects also had suspicious appearing optic discs, making it more difficult for the diagnostic test to differentiate them from diseased subjects. A study by Medeiros et al²⁵ evaluating the impact of design-related bias in studies of diagnostic tests in glaucoma found that studies with a case-control design including patients with well-established disease and a separate group of normal (unsuspected) control subjects resulted in substantial overestimation of the performance of the tests.

We used evidence of previously documented progressive optic disc change as the reference standard to classify glaucoma suspect patients as disease positive versus disease negative. In the absence of visual field loss, glaucoma can be diagnosed with certainty only by

demonstrating a history of progressive glaucomatous changes to the optic nerve. This approach was first proposed by Medeiros et al²⁴ for evaluation of diagnostic tests in glaucoma. Presence of progressive optic disc damage is also highly predictive of future development of visual field defects.³⁷ However, although it enables the evaluation of diagnostic accuracy in a situation that better resembles clinical practice, it still has some limitations. It is possible, for example, that some patients that had glaucomatous optic disc damage were not included because they did not present with progressive damage during the follow-up period. Patients with suspicious optic disc appearance who did not show any evidence of optic disc change or visual field loss during follow-up were considered as controls. It might be argued that some of these patients from the control group could have had glaucomatous damage to the optic disc or might develop visual field defects, but the follow-up time was insufficient to detect progression. Although it is unlikely that glaucoma patients would not progress or develop functional loss followed untreated for an average of 14 years, this possibility cannot be completely excluded. Another limitation of this study design is that stereophotograph evaluation of optic disc change has an imperfect inter-observer agreement.³⁸ As a consequence, some eyes could be misdiagnosed and incorrectly designated to the glaucomatous or to the control group. However, in order to minimize misclassifications, we required consensus grading by 2 trained expert ophthalmologists and a third experienced grader reviewed the stereophotographs in cases of disagreement.

In the present study, the Spectralis SDOCT parameters with highest diagnostic accuracies were the temporal superior, global and temporal inferior RNFL thickness measurements, with AUCs of 0.88, 0.86 and 0.81, respectively. RNFL losses in the temporal superior and temporal inferior sectors are expected and correspond to initial stages of optic nerve damage in patients with glaucoma.^{12, 18, 39} The poor performance of the temporal and nasal sectors can be justified by the fact that those sectors are more frequently affected in advanced glaucoma and our population is composed mostly of individuals with early damage. Retinal nerve fiber layer parameters performed significantly better than topographic parameters in differentiating glaucomatous and control eyes. Temporal superior average RNFL thickness was the parameter with the best performance for the Spectralis SDOCT, with an AUC of 0.88; whereas rim area was the parameter with the best performance for the CSLO, with an AUC of 0.72. Given the selection criteria of our study, these results are not surprising and are similar to those found in a previous study comparing RNFL assessment by scanning laser polarimetry with CSLO.²² The difference in ancestry between groups was marginally significant in our study. Although previous studies reported that ancestry did not influence the diagnostic performance of the SDOCT technology⁴⁰, we performed an additional analysis excluding black patients. As expected, similar results were achieved, with SDOCT temporal superior RNFL thickness performing better than CSLO rim area (0.87 vs 0.73; $p = 0.031$).

The starting point of a diagnostic process occurs when a clinician combines the medical history with clinical examination to estimate the probability of the presence of the disease, also known as pretest probability. The results of diagnostic tests are then used to modify the pretest probability of disease yielding a new posttest probability. The direction and magnitude of this change from pretest to posttest are determined by the test's properties, in particular by the likelihood ratio of the test. The LR represents the magnitude of change from a clinician's initial suspicion for disease (pretest probability) to the likelihood of disease after the test result (posttest probability). In our study, outside normal limits results for Spectralis SDOCT parameters were generally associated with large changes from the pretest to posttest probability of disease. In contrast, outside normal limits results for the HRT-III MRA were only associated with insignificant to small effects. This means that an abnormal result on Spectralis SDOCT would have a larger impact in increasing the probability of disease than an abnormal result found on the MRA provided by the CSLO.

For within normal limits, the LR for the overall Spectralis SDOCT classification was smaller (i.e., better) than the overall classification for MRA (0.26 vs 0.42; respectively), indicating that normal results on SDOCT would carry more impact in excluding the disease than those from CSLO. The evaluation of the integrity of the RNFL during clinical examination is difficult, especially in older patients with light pigmented retinas or hazy optical media. On the other hand, evaluation of the optic nerve and identification of areas of suspicious rim thinning or optic disc cupping is more straightforward. Therefore, patients with suspicious disc appearance will generally be those with large cups or suspicious rim thinning. In these patients, it is not surprising that topographic information about cup size or cup depth, for example, does not provide much additional information in terms of establishing the definitive diagnosis.

The design of our study evaluates a diagnostic test in a scenario that resembles the use of imaging devices in clinical practice for assisting in detecting damage in patients suspected of having glaucoma. However, this design might not be the most appropriate for other situations, such as when assessing the ability of an instrument to screen for patients with glaucomatous visual field loss in the general population. Therefore, the study design should take into account the context and clinical situation where the diagnostic test will be applied. In addition, it should be noted that longitudinal follow-up of glaucoma suspects and glaucoma patients may represent the most advantageous use of these technologies in clinical practice.^{23, 24} In fact, in many glaucoma suspects, confirmation about the presence or absence of disease will only be possible after careful long-term follow-up and imaging devices could be used to monitor structural changes in this situation.

In conclusion, our results showed that RNFL imaging with Spectralis SDOCT performed well in detecting preperimetric glaucomatous damage in subjects who were suspected of having the disease, presenting a better diagnostic capability than topographic assessment with the CSLO. Abnormal results on SDOCT (as compared to the instrument's normative database) were associated with high likelihood ratios and large effects on posttest probabilities of having preperimetric glaucomatous damage.

Acknowledgments

Supported in part by NIH/NEI grants EY021818 (FAM), EY11008 (LMZ), EY14267 LMZ), CAPES grand BEX 1066/11-0, an unrestricted grant from Research to Prevent Blindness (New York, NY), Grant for participants' glaucoma medications from Alcon, Allergan, Pfizer, Merck and Santen.

References

1. Nassif N, Cense B, Park B, et al. In vivo high-resolution video-rate spectral-domain optical coherence tomography of the human retina and optic nerve. *Opt Express* [serial online]. 2004; 12:367–76. Available at: <http://www.opticsinfobase.org/oe/abstract.cfm?uri=oe-12-3-367>.
2. Wojtkowski M, Srinivasan V, Ko T, et al. Ultrahigh-resolution, high-speed, Fourier domain optical coherence tomography and methods for dispersion compensation. *Opt Express* [serial online]. 2004; 12:2404–22. Available at: <http://www.opticsinfobase.org/oe/abstract.cfm?uri=oe-12-11-2404>.
3. Mistlberger A, Liebmann JM, Greenfield DS, et al. Heidelberg retina tomography and optical coherence tomography in normal, ocular-hypertensive, and glaucomatous eyes. *Ophthalmology*. 1999; 106:2027–32. [PubMed: 10519603]
4. Zangwill LM, Bowd C, Berry CC, et al. Discriminating between normal and glaucomatous eyes using the Heidelberg Retina Tomograph, GDx Nerve Fiber Analyzer, and Optical Coherence Tomograph. *Arch Ophthalmol*. 2001; 119:985–93. [PubMed: 11448320]
5. Greaney MJ, Hoffman DC, Garway-Heath DF, et al. Comparison of optic nerve imaging methods to distinguish normal eyes from those with glaucoma. *Invest Ophthalmol Vis Sci*. 2002; 43:140–5. [PubMed: 11773024]

6. Medeiros FA, Zangwill LM, Bowd C, Weinreb RN. Comparison of the GDx VCC scanning laser polarimeter, HRT II confocal scanning laser ophthalmoscope, and Stratus OCT optical coherence tomograph for the detection of glaucoma. *Arch Ophthalmol*. 2004; 122:827–7. [PubMed: 15197057]
7. Jindal S, Dada T, Sreenivas V, et al. Comparison of the diagnostic ability of Moorfield's regression analysis and glaucoma probability score using Heidelberg retinal tomograph III in eyes with primary open angle glaucoma. *Indian J Ophthalmol*. 2010; 58:487–92. [PubMed: 20952832]
8. Rao HL, Babu GJ, Sekhar GC. Comparison of the diagnostic capability of the Heidelberg retina tomographs 2 and 3 for glaucoma in the Indian population. *Ophthalmology*. 2010; 117:275–81. [PubMed: 19969365]
9. Naithani P, Sihota R, Sony P, et al. Evaluation of optical coherence tomography and Heidelberg retinal tomography parameters in detecting early and moderate glaucoma. *Invest Ophthalmol Vis Sci*. 2007; 48:3138–45. [PubMed: 17591883]
10. Medeiros FA, Zangwill LM, Bowd C, et al. Evaluation of retinal nerve fiber layer, optic nerve head, and macular thickness measurements for glaucoma detection using optical coherence tomography. *Am J Ophthalmol*. 2005; 139:44–55. [PubMed: 15652827]
11. Wang X, Li S, Fu J, et al. Comparative study of retinal nerve fibre layer measurement by RTVue OCT and GDx VCC. *Br J Ophthalmol*. 2011; 95:509–13. [PubMed: 20657017]
12. Park SB, Sung KR, Kang SY, et al. Comparison of glaucoma diagnostic capabilities of Cirrus HD and Stratus optical coherence tomography. *Arch Ophthalmol*. 2009; 127:1603–9. [PubMed: 20008715]
13. Chang RT, Knight OJ, Feuer WJ, Budenz DL. Sensitivity and specificity of time-domain versus spectral-domain optical coherence tomography in diagnosing early to moderate glaucoma. *Ophthalmology*. 2009; 116:2294–9. [PubMed: 19800694]
14. Parikh RS, Parikh S, Sekhar GC, et al. Diagnostic capability of optical coherence tomography (Stratus OCT 3) in early glaucoma. *Ophthalmology*. 2007; 114:2238–43. [PubMed: 17561260]
15. Hougaard JL, Heijl A, Bengtsson B. Glaucoma detection by Stratus OCT. *J Glaucoma*. 2007; 16:302–6. [PubMed: 17438424]
16. Leung CK, Cheung CY, Weinreb RN, et al. Retinal nerve fiber layer imaging with spectral-domain optical coherence tomography: a variability and diagnostic performance study. *Ophthalmology*. 2009; 116:1257–63. [PubMed: 19464061]
17. Rao HL, Zangwill LM, Weinreb RN, et al. Comparison of different spectral domain optical coherence tomography scanning areas for glaucoma diagnosis. *Ophthalmology*. 2010; 117:1692–9. [PubMed: 20493529]
18. Sehi M, Grewal DS, Sheets CW, Greenfield DS. Diagnostic ability of Fourier-domain vs time-domain optical coherence tomography for glaucoma detection. *Am J Ophthalmol*. 2009; 148:597–605. [PubMed: 19589493]
19. Leung CK, Ye C, Weinreb RN, et al. Retinal nerve fiber layer imaging with spectral-domain optical coherence tomography: a study on diagnostic agreement with Heidelberg Retinal Tomograph. *Ophthalmology*. 2010; 117:267–74. [PubMed: 19969364]
20. Leung CK, Lam S, Weinreb RN, et al. Retinal nerve fiber layer imaging with spectral-domain optical coherence tomography: analysis of the retinal nerve fiber layer map for glaucoma detection. *Ophthalmology*. 2010; 117:1684–91. [PubMed: 20663563]
21. Leite MT, Rao HL, Zangwill LM, et al. Comparison of the diagnostic accuracies of the Spectralis, Cirrus, and RTVue optical coherence tomography devices in glaucoma. *Ophthalmology*. 2011; 118:1334–9. [PubMed: 21377735]
22. Medeiros FA, Vizzeri G, Zangwill LM, et al. Comparison of retinal nerve fiber layer and optic disc imaging for diagnosing glaucoma in patients suspected of having the disease. *Ophthalmology*. 2008; 115:1340–6. [PubMed: 18207246]
23. Medeiros FA. How should diagnostic tests be evaluated in glaucoma? *Br J Ophthalmol*. 2007; 91:273–4. [PubMed: 17322462]
24. Medeiros FA, Zangwill LM, Bowd C, et al. Use of progressive glaucomatous optic disk change as the reference standard for evaluation of diagnostic tests in glaucoma. *Am J Ophthalmol*. 2005; 139:1010–8. [PubMed: 15953430]

25. Medeiros FA, Ng D, Zangwill LM, et al. The effects of study design and spectrum bias on the evaluation of diagnostic accuracy of confocal scanning laser ophthalmoscopy in glaucoma. *Invest Ophthalmol Vis Sci.* 2007; 48:214–22. [PubMed: 17197535]
26. Leite MT, Rao HL, Weinreb RN, et al. Agreement among spectral-domain optical coherence tomography instruments for assessing retinal nerve fiber layer thickness. *Am J Ophthalmol.* 2011; 151:85–92. [PubMed: 20970108]
27. Swindale NV, Stjepanovic G, Chin A, Mikelberg FS. Automated analysis of normal and glaucomatous optic nerve head topography images. *Invest Ophthalmol Vis Sci.* 2000; 41:1730–42. [PubMed: 10845593]
28. Wollstein G, Garway-Heath DF, Hitchings RA. Identification of early glaucoma cases with the scanning laser ophthalmoscope. *Ophthalmology.* 1998; 105:1557–63. [PubMed: 9709774]
29. Dodd LE, Pepe MS. Partial AUC estimation and regression. *Biometrics.* 2003; 59:614–23. [PubMed: 14601762]
30. Zhou, XH.; Obuchowski, NA.; McClish, DK. *Statistical Methods in Diagnostic Medicine.* New York: Wiley; 2002. p. 274-306.
31. Alonzo TA, Pepe MS. Distribution-free ROC analysis using binary regression techniques. *Biostatistics.* 2002; 3:421–32. [PubMed: 12933607]
32. Radack KL, Rouan G, Hedges J. The likelihood ratio: an improved measure for reporting and evaluating diagnostic test results. *Arch Pathol Lab Med.* 1986; 110:689–93. [PubMed: 3755325]
33. Jaeschke R, Guyatt GH, Sackett DL. Evidence-Based Medicine Working Group. Users' guides to the medical literature. III. How to use an article about a diagnostic test. B. What are the results and will they help me in caring for my patients? *JAMA.* 1994; 271:703–7. [PubMed: 8309035]
34. Fagan TJ. Letter: Nomogram for Bayes theorem. *N Engl J Med.* 1975; 293:257. [PubMed: 1143310]
35. Simel DL, Samsa GP, Matchar DB. Likelihood ratios with confidence: sample size estimation for diagnostic test studies. *J Clin Epidemiol.* 1991; 44:763–70. [PubMed: 1941027]
36. Lijmer JG, Mol BW, Heisterkamp S, et al. Empirical evidence of design-related bias in studies of diagnostic tests. *JAMA.* 1999; 282:1061–6. [PubMed: 10493205]
37. Medeiros FA, Alencar LM, Zangwill LM, et al. Prediction of functional loss in glaucoma from progressive optic disc damage. *Arch Ophthalmol.* 2009; 127:1250–6. [PubMed: 19822839]
38. Breusegem C, Fieuws S, Stalmans I, Zeyen T. Agreement and accuracy of non-expert ophthalmologists in assessing glaucomatous changes in serial stereo optic disc photographs. *Ophthalmology.* 2011; 118:742–6. [PubMed: 21055815]
39. Moreno-Montanes J, Olmo N, Alvarez A, et al. Cirrus high-definition optical coherence tomography compared with Stratus optical coherence tomography in glaucoma diagnosis. *Invest Ophthalmol Vis Sci.* 2010; 51:335–43. [PubMed: 19737881]
40. Girkin CA, Liebmann J, Fingeret M, et al. The effects of race, optic disc area, age, and disease severity on the diagnostic performance of spectral-domain optical coherence tomography. *Invest Ophthalmol Vis Sci.* 2011; 52:6148–53. [PubMed: 21421879]

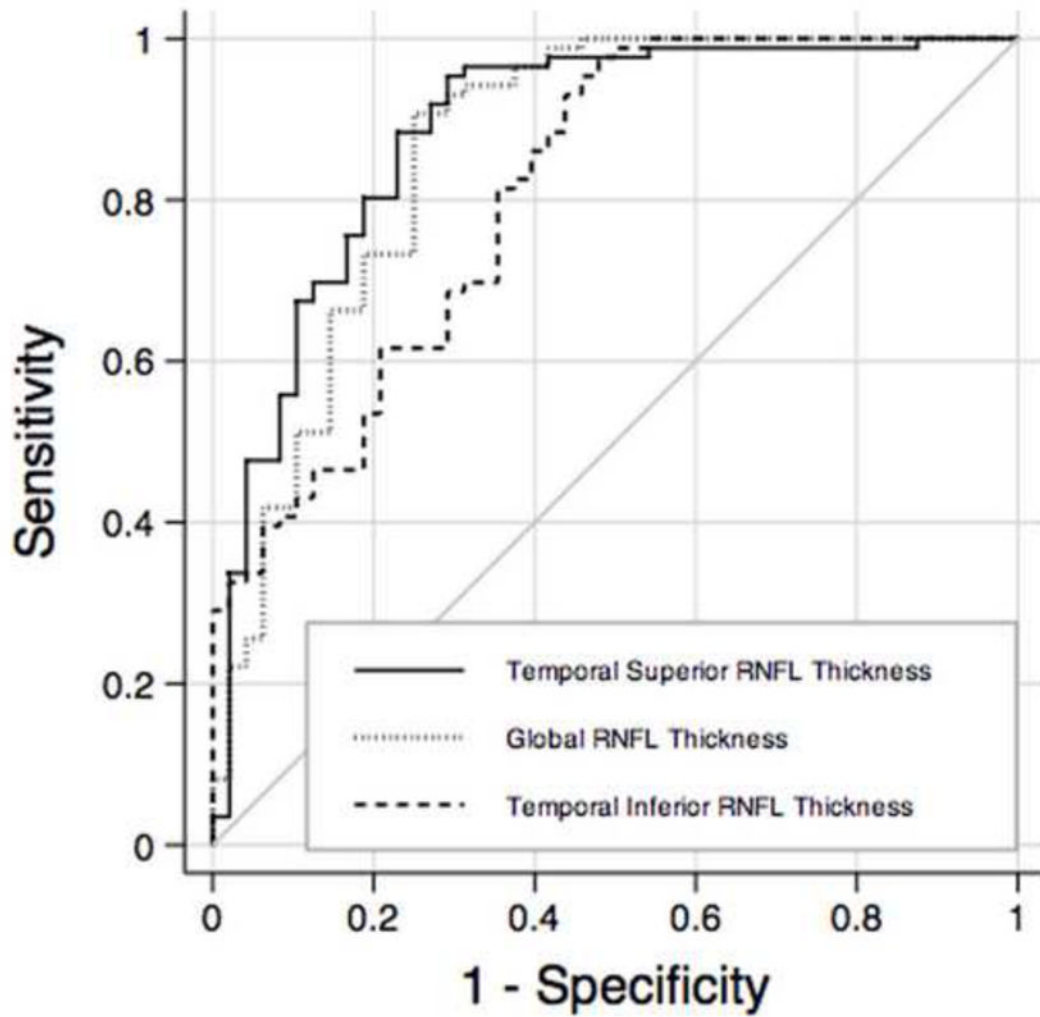


FIGURE 1. Receiver operating characteristics for temporal superior thickness, global thickness and temporal inferior thickness obtained by spectral domain optical coherence tomography. RNFL = retinal nerve fiber layer.

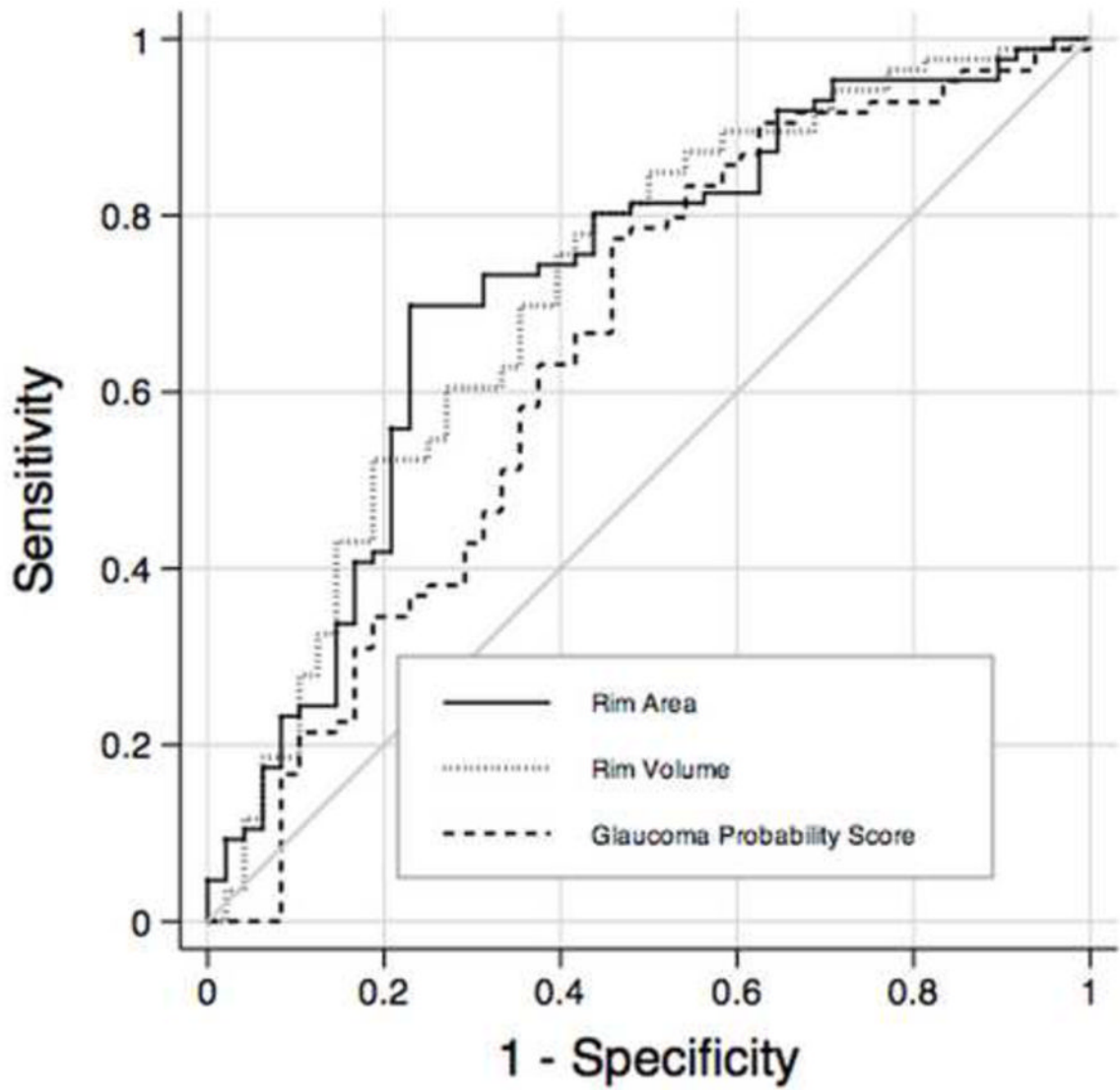


FIGURE 2. Receiver operating characteristics curves for rim volume, rim area and glaucoma probability score parameters obtained by confocal scanning laser ophthalmoscopy. RNFL = retinal nerve fiber layer.

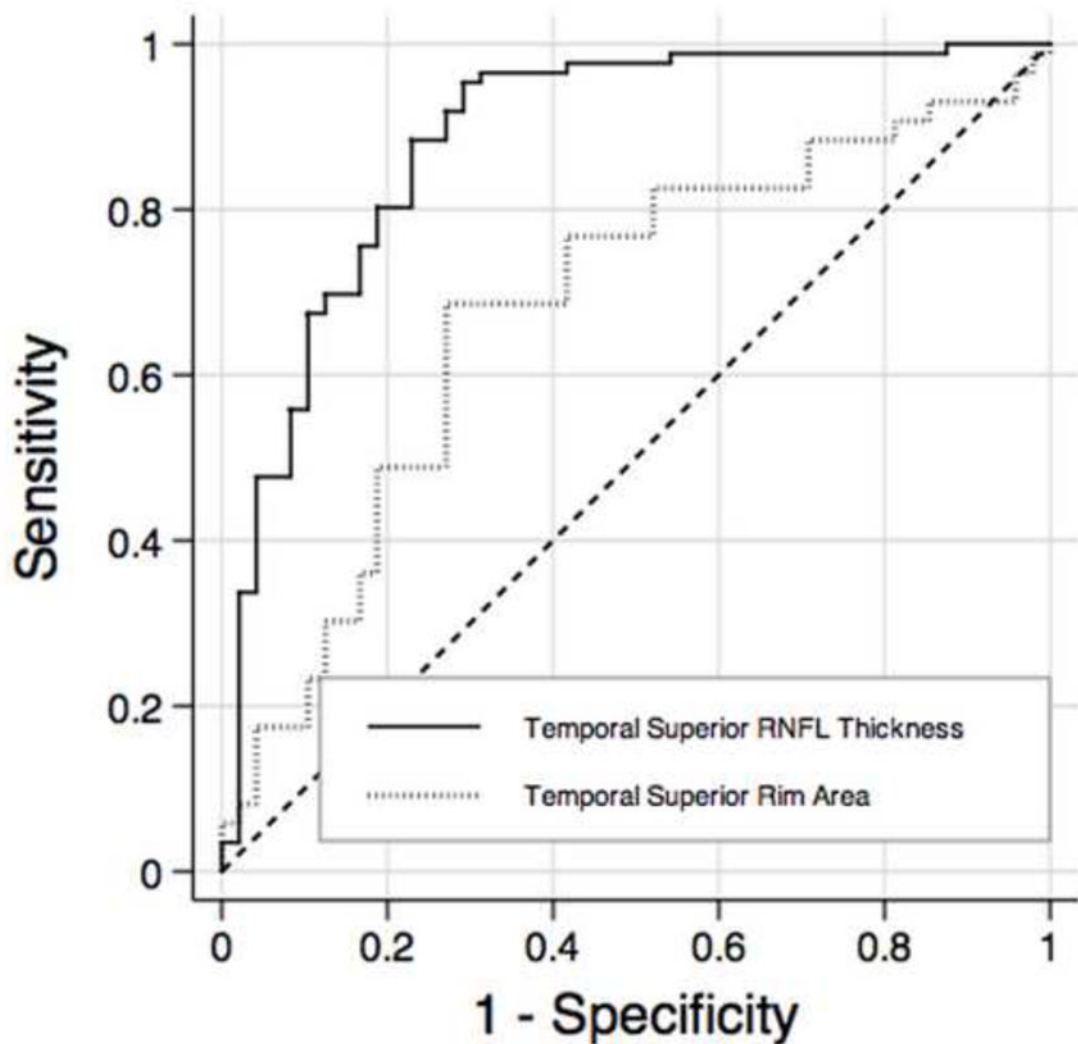


FIGURE 3.

Receiver operating characteristics curves for temporal superior thickness obtained by spectral domain optical coherence tomography and temporal superior rim area obtained by confocal scanning laser ophthalmoscopy. RNFL = retinal nerve fiber layer.

Table 1

Demographic and clinical characteristics of the preperimetric glaucoma and control study groups

Characteristics	Glaucoma (n=48)	Control (n=86)	P Value
Age, years *	66.1 ± 9.3	63.6 ± 10.8	0.238
Gender, % male	50.0	32.6	0.097
Ancestry, % African-American	16.6	4.3	0.057
MD, dB †	-0.63 ± 1.24	0.09 ± 1.33	0.002
PSD, dB †	1.61 (1.43, 1.56, 1.77)	1.55 (1.28, 1.46, 1.70)	0.136
Disc area, mm ² *	1.97 ± 0.08	1.97 ± 0.06	0.927
Intraocular pressure, mmHg *	19.77 ± 0.56	19.97 ± 0.70	0.825
Signal strength of the Spectralis SDOCT images *	23.95 ± 0.53	23.58 ± 0.42	0.582
Quality of the HRT-III images, sd †	18.31 (13, 18, 20.5)	17.31(13, 15, 20)	0.212
Follow-up, years *	14.0 ± 3.6	14.9 ± 4.2	0.466
Ametropia, diopters *	-0.81 ± 0.30	-0.70 ± 0.27	0.795
Axial length, mm *	24.09 ± 0.16	24.01 ± 0.15	0.709
Average corneal curvature, mm *	7.72 ± 0.04	7.78 ± 0.03	0.274
Pachymetry, μm *	569.74 ± 6.49	579.14 ± 5.93	0.288

MD = mean deviation

PSD = pattern standard deviation

dB = decibels

SDOCT = spectral domain optical coherence tomography

sd = standard deviation

* Normally distributed variables; represented by mean (standard deviation).

† Non-normally distributed variables; represented by mean (first quartile, median, third quartile).

Table 2

Mean \pm standard deviation values of spectral domain optical coherence tomography RNFL parameters with area under the receiver operating characteristics curves and sensitivities at fixed specificities for discriminating between preperimetric glaucoma and control groups

Parameter	Glaucoma (n=48)	Control (n=86)	P Value*	AUC (SE)	Sensitivity (Specificity = 80%)	Sensitivity (Specificity = 95%)
Temporal superior thickness	102.0 \pm 3.3	128.8 \pm 2.0	< 0.001	0.88 (0.03)	80.2%	47.6%
Global thickness	78.2 \pm 2.0	92.8 \pm 1.2	< 0.001	0.86 (0.03)	73.2%	25.5%
Temporal inferior thickness	109.2 \pm 4.0	136.3 \pm 2.1	< 0.001	0.81 (0.04)	53.4%	33.7%
Nasal superior thickness	79.3 \pm 3.6	93.0 \pm 2.2	< 0.001	0.73 (0.05)	34.8%	15.1%
Nasal thickness	59.7 \pm 2.6	69.6 \pm 1.5	< 0.001	0.70 (0.05)	38.3%	15.1%
Nasal inferior thickness	88.1 \pm 4.3	106.0 \pm 3.2	< 0.001	0.68 (0.04)	37.2%	25.5%
Temporal thickness	63.2 \pm 2.8	69.0 \pm 1.5	0.04	0.62 (0.05)	27.9%	15.1%

RNFL = retinal nerve fiber layer

AUC = area under the receiver operating characteristic curve

SE = standard error

* For comparison of mean values of spectral domain optical coherence tomography parameters between glaucomatous and control eyes

Table 3

Likelihood ratios and 95% confidence intervals for spectral domain optical coherence tomography parameters

Parameter	Within Normal Limits	Borderline	Outside Normal Limits
Temporal superior thickness	0.44 (0.12 to 0.77)	21.50 (19.49 to 23.50)	26.87 (24.88 to 28.86)
Global thickness	0.39 (0.02 to 0.76)	5.37 (4.29 to 6.45)	Infinity (NA)
Temporal inferior thickness	0.48 (0.18 to 0.78)	21.50 (19.49 to 23.50)	Infinity (NA)
Nasal superior thickness	0.71 (0.50 to 0.92)	4.30 (3.31 to 5.28)	7.16 (5.00 to 9.32)
Nasal thickness	0.89 (0.78 to 1.00)	4.47 (2.87 to 6.08)	Infinity (NA)
Nasal inferior thickness	0.92 (0.83 to 1.01)	0.92 (0.83 to 1.01)	Infinity (NA)
Temporal thickness	0.82 (0.66 to 0.99)	2.09 (1.05 to 3.12)	Infinity (NA)
Overall classification	0.26 (0 to 0.82)	1.05 (0.35 to 1.75)	50.16 (48.20 to 52.12)

NA = not applicable

Table 4

Mean \pm standard deviation values of confocal scanning laser ophthalmoscopy parameters with areas under the receiver operating characteristic curves and sensitivities at fixed specificities for discriminating between preperimetric glaucoma and control groups

Parameter	Glaucoma (n=48)	Control (n=86)	P Value*	AUC (SE)	Sensitivity (Specificity = 80%)	Sensitivity (Specificity = 95%)
Rim area (mm ²)	1.20 \pm 0.05	1.38 \pm 0.03	< 0.001	0.72 (0.05)	41.8%	10.4%
Rim volume (mm ³)	0.30 \pm 0.02	0.38 \pm 0.01	0.002	0.71 (0.05)	52.3%	11.6%
Linear cup-to-disk ratio	0.59 \pm 0.02	0.52 \pm 0.01	0.002	0.66 (0.05)	41.6%	25.0%
Cup-to-disk area ratio	0.36 \pm 0.02	0.28 \pm 0.01	0.003	0.66 (0.05)	41.6%	22.9%
Rim-to-disk area ratio	0.63 \pm 0.02	0.71 \pm 0.01	0.003	0.66 (0.05)	29.0%	6.9%
RNFL CSA (mm ²)	1.07 \pm 0.07	1.29 \pm 0.05	0.005	0.65 (0.05)	38.3%	17.4%
Global GPS	0.54 \pm 0.05	0.38 \pm 0.03	0.006	0.64 (0.05)	45.8%	16.6%
Mean RNFL thickness (mm)	0.22 \pm 0.01	0.26 \pm 0.01	0.004	0.64 (0.05)	36.0%	9.3%
Cup area (mm ²)	0.78 \pm 0.08	0.59 \pm 0.04	0.023	0.62 (0.06)	37.5%	18.7%
Cup volume (mm ³)	0.24 \pm 0.04	0.14 \pm 0.01	0.016	0.62 (0.05)	35.4%	16.6%
Mean cup depth (mm)	0.28 \pm 0.02	0.25 \pm 0.01	0.071	0.58 (0.06)	33.3%	10.4%

RNFL = retinal nerve fiber layer

AUC = area under the receiver operating characteristic curve

SE = standard error

RNFL CSA = retinal nerve fiber layer cross sectional area

Global GPS = global glaucoma probability score

* For comparison of mean values of confocal scanning laser ophthalmoscopy parameters between glaucomatous and control eyes

Table 5

Likelihood ratios and 95% confidence intervals for confocal scanning laser ophthalmoscopy Moorfields Regression Analysis

Parameter	Within Normal Limits	Borderline	Outside Normal Limits
Temporal superior	0.71 (0.46 to 0.95)	2.50 (1.77 to 3.23)	2.98 (1.59 to 4.37)
Global	0.59 (0.29 to 0.89)	2.32 (1.58 to 3.07)	4.92 (3.83 to 6.01)
Temporal inferior	0.50 (0.17 to 0.84)	2.76 (2.09 to 3.44)	17.91 (15.89 to 19.94)
Nasal superior	0.66 (0.39 to 0.92)	2.86 (1.80 to 3.92)	3.32 (2.47 to 4.17)
Nasal	0.77 (0.53 to 1.02)	0.89 (0 to 1.90)	3.32 (2.47 to 4.17)
Nasal inferior	0.61 (0.28 to 0.94)	1.15 (0.39 to 1.91)	3.80 (3.04 to 4.56)
Temporal	0.86 (0.70 to 1.01)	2.55 (1.66 to 3.45)	1.79 (0 to 4.54)
Overall classification	0.42 (0 to 0.98)	0.82 (0.24 to 1.41)	3.19 (2.64 to 3.75)

Table 6

Areas under the receiver operating characteristics curves \pm standard error of spectral domain optical coherence tomography retinal nerve fiber layer parameters and confocal scanning laser ophthalmoscopy rim area by sectors

Sector	SDOCT	CSLO	P value
Temporal superior	0.88 \pm 0.03	0.68 \pm 0.05	0.001
Temporal inferior	0.81 \pm 0.04	0.64 \pm 0.05	0.01
Nasal superior	0.73 \pm 0.05	0.67 \pm 0.05	0.40
Nasal	0.70 \pm 0.05	0.66 \pm 0.05	0.52
Nasal inferior	0.68 \pm 0.04	0.61 \pm 0.05	0.27
Temporal	0.62 \pm 0.05	0.60 \pm 0.05	0.75

SDOCT = spectral domain optical coherence tomography

CSLO = confocal scanning laser ophthalmoscopy